Swelling properties of Ultra-violet Cured Unsaturated Polyester Resin Reinforced with Kenaf Fiber Composites

Soad Alsheheri

Chemistry Department, King Abdulaziz University, Jeddah, Saudi Arabia.

ARTICLE INFO

ABSTRACT

Polyester resins are cost-beneficial thermoset material which are frequently used because of their exemplary processability, cross-linking tendency, and mechanical properties. Also, when cured they become more useful as their properties are modified during curing. Polyester resins offer attractive mechanical properties when reinforced with natural fibers. In this study, the factors that affect the polymer-solvent relationship of the product which were photofabricated and ultraviolet radiation curing of Unsaturated Polyester Resin Composites (UPRC) are discussed. UPRC was prepared utilizing kenaf fiber (reinforcing agent) and unsaturated polyester resins (matrix) with styrene IRGACURE 1800 was used as photo-initiator. Palm oil–based unsaturated polyester resins were synthesized using different proportions of Monoglyceride (MG) /Maleic Anhydride (MA) through the interaction of the appropriate MG monomer with varying equivalents of MA, using 2-methylimidazole as a catalyst. The gelation of nanocomposites ranged from 89% to 95%. The percentage of void of the composites range from 9.4 (±0.46%) for UPRCc and 12.4 (±0.52%) for UPRCd. The n values for nanocomposites are ranged from 0.52 – 0.56 in DMF and from 0.54 – 0.61 in toluene. The n values are indicative of Fickian sorption mechanism.

1. Introduction

"The curing of polyester resins modify their properties and make them more useful and cost-beneficial thermoset material [1,2]. The mechanical properties of polyesters make them useful in industrial and domestic applications especially when reinforced with fibers or fillers. Natural fiber-reinforced polymers are abundantly used in construction and automotive industries [3-6]. The reinforcement with natural fibers make them to possess numerous advantageous properties, e.g., cost effectiveness, lightweight, high specific properties, and ability to synthesize via renewable resources.

The fibrous polymer composite was composed of fibers, matrix and interface [7]. The mechanical properties of the composites vary with the strength and the elasticity of fibers, matrices, and the fiber–matrix bond that controls the stress transfer [8, 9]. The stress transfer between the fiber and the matrix is diminished when the binding force is weaker between the fiber and matrix [9]. Studies of glass fiber–reinforced thermosets are dedicated on interface behavior characterization and manipulating the interface [8–12] and the influence of fiber–matrix interface on composite materials' mechanical aspects assessed through different models [9]. In a previous work, [13] of unsaturated polyester composites' mechanical properties which were strengthened with different natural fibers (jute, sisal, and flax) and glass fiber were analyzed. Studies indicate jute composites maintained the best flexural and tensile strength values but the lowest impact results as a consequence of the higher interface adhesion. Alternatively, sisal fiber composites exhibited the least mechanical and hydrophobic properties. Composites made from woven jute and non-woven flax maintained similar tensile and flexural aspects and rate of water absorption. Apart from cost efficiency and mechanical aspects, it is vital to analyze flame retardant behavior of materials used for construction industry applications.

Current developments in irradiation devices, photoinitiators, and photoreactive multifunctional telechelic oligomers and monomers evolved the curing technology in the adhesive and coatings industries. Current advancements showcase UV curing advantages require the curing of thick composites. Photo-polymerization is the curing process involving transforming liquid or low-melting solid oligomers to crosslinked durable products under the influence of ultraviolet radiation. The process of photochemical UV-curing comprises irradiating a mixture of liquid oligomers, monomers, and a small number of photoinitiators. When the mixture, was exposed to UV light, it hardens immediately and becomes a sturdy transparent product. The end product could be adhesives, decorative printing inks, and polymer matrices in a composite material. UV-curable systems offer two options: (i) a process effected by a free-radical photoinitiator and (ii) by cationic photoinitiators. The UV-cured systems were considered for altering cures of thin layers of adhesives and coatings. The intensity reduction of UV light when radiation get through thick sections makes this technology restricted to cure thin layers only. The studies on photo-fabrication of bio-fiber composites is still somehow an uncharted territory. Currently, biofiber-based composites are created through a thermally curable process. UV radiation curing outperforms thermal curing because of the following reasons: (i) UV light curing is very fast, allowing for enhanced output, (ii) UV-curable preparations are "single pack" systems that has longer stability when compared with ambient temperature–curable "two-pack" systems using ethyl methyl ketone peroxide where curing do not occur when the resin was not exposed to UV radiation. Viscosity of formulations remain unchanged during resin application and mat impregnation. The product's consistent quality can be guaranteed and lessening of the wastage of "in-process" resinous materials is also attainable, (iii) UV curing is ecologically benign, energy, time and space efficient , (iv) utilization of appropriate choice of UV lamps and photoinitiators, a uniform and consistent "through-cure" is achievable, (v) UV curing occurs without peroxides unlike in traditional curing systems, (vi) and curing reaction goes to near completion, without any residual styrene in the end product , a desirable characteristic which cannot be achieved in peroxide-based curing systems.

The commercial use of polyesters gained popularity as very useful industrial polymers possessing interesting mechanical properties. The effect of different acids, bases and certain solvents bring the changes in the structure of polyesters. The use of polyesters in food, beverages packing industry influences human and domestic animal life. The polyester containers are widely used in storing oils, food, water, organic solvents etc. The structure of polyester and the properties and structure of various solvents create effect on swelling of the polymers.

Also, the temperature and storing time do influence the swelling property of polyesters [14].

This article focuses on solubility and polymer–solvent interaction parameters for photofabricated biofiber composites that contains unsaturated polyester resin as matrix and kenaf fiber. UV light was used for implementation of the composites curing. The composites' void content was determined prior to swelling tests to displace the free solvent present in the system.

2. Results and discussion

Lignocellulosic materials usage in crafting composites has garnered quite the attention, attributed to numerous advantages made possible by lignocellulosic fillers, e.g., greater deformability, biodegradability, lower density and cost, and less abrasiveness to equipments. However, the main obstacle facing the creation of a good-polymer composite, in terms of physical and mechanical aspects, is the lignocellulosic material–polymer matrix compatibility. Lignocellulosic materials–made building products, contributes to the construction industry (specifically decking) as it is more cost effective compared with natural wood. The making of interior automotive products, are constructed from natural fibers, like hemp, flax, kenaf, or jute, reinforcing numerous thermoplastics and thermosets. These lignocellulosic materials applications are mainly directed towards replacing glass fibers in reinforced plastics. It offers various advantages inherent to natural fibers acting reinforcement materials: being light weight, of low price, and recyclable. Nonetheless, concerning optimal lignocellulose-based composites, stress transfer's mechanism and efficiency between the components usually influence the composite's performance. This transition region is dubbed the interface. The possible chemical interactions between the components in the interface, the properties of the composite will be enhanced, for example, this happens in the case of lignocellulosic fiber–based Unsaturated Polyester Resin (UPR). However, these biofibers composites require the synthesis of monomer and polymers matrix as precursors before proceeding with the fabrication of the nanocomposite.

2.1. Photo-fabrication of UPRC$_{a-d}$

MG monomer was first synthesized by the reaction of glycerol and palm oil with using sodium hydroxide catalyst. Palm oil based UPR was made using various MG: MA ratios as described elsewhere [15] by the reaction between MG monomer with varying equivalents of maleic anhydride, using 2-methylimidazole as a catalyst. Table 1 illustrates the symbols and chemical compositions for the fabricated UPRC$_{a-d}$. Table 1 demonstrates the chemical composition for the required unsaturated polyester resin.

Table 1: Symbols and chemical compositions for UPRC$_{a-d}$.

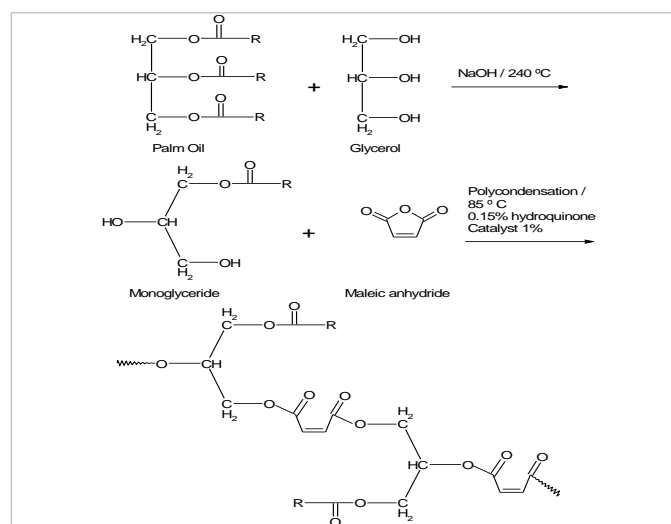| Composite Symbol	MG (eq.)	Yield (%)
UPRCa	1	2
UPRCb	1	3
UPRCc	1	4
UPRCd	1	5

Figure 1. Scheme for synthesis of Unsaturated polyester resin.

Afterward, UPRC$_{a-d}$ biofiber composites of different formulations were crafted by ultraviolet curing technique in the presence of styrene, a kenaf fiber mat, and free radical initiator IRGACURE 1800. IRGACURE 1800 photoinitiator chemical structures are illustrated in figure 2. The figure 3 demonstrates the scheme for synthesis of UPRCa-d nanocomposites.
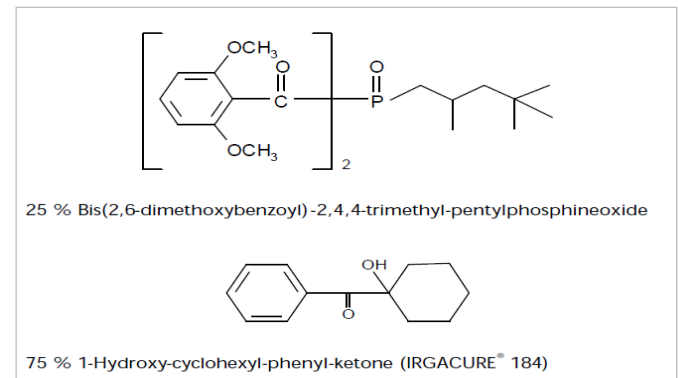

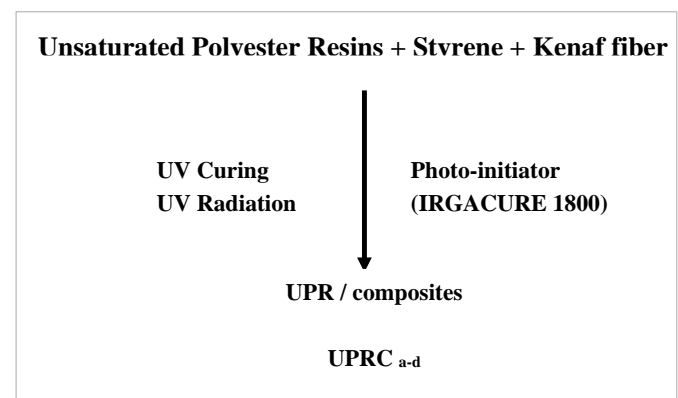**Figure 2.** Chemical structures for IRGACURE 1800.

Figure 3. Schematic diagram of UPRC$_{a-d}$ synthesis.

2.2. Swelling Performance

The extent of curing of synthesized UPRC nanocomposites is measured by ASTM D2765. The percentage of gelation for the fabricated nanocomposites is given in Table 2. The test was performed by Soxhlet extraction with toluene as solvent. The cured nanocomposites were placed in a cellulose extraction thimble in the Soxhlet's extractor. Three sets of Soxhlet's extractors were used. The extraction of solvents was carried out with 200 mL toluene for four hours. After that, the taken samples were subjected to vacuum drying and re-weighed until they reached a constant weight. The gel content of the coating was assessed per the equation below:

Gel content % (w_2 / w_1) x 100

Here w_1 and w_2 illustrate the weights before and after extraction, respectively. Table 2 data give us an impression about the fabricated materials' gelation performance. All UPRC compositions attained high gel content of more than 90% while UPRC$_a$ which maintains 89.05% content value. UPRC$_c$ shows a largest gel content value of 95.49%. Gel content values for all UPRC formulations ranks as follows: UPRC$_c$ > UPRC$_b$ > UPRC$_d$ > UPRC$_a$. The larger the gel content, the larger the degree of curing in the biofiber formulation, prepared by the use of the higher equivalent of MA content and the higher degree of crosslinking. Gel fraction increases with increase in MA up to a ratio of MG to MA of 1: 4 (eq./eq.) for UPRC$_c$, while gel fraction decreases for the last formulation at a 1: 5 (eq./eq.) ratio, attributable to the unsaturated groups pre reaction during the resin preparation.

Table 2: The gelation percent for the fabricated UPRC$_{a-d}$ nanocomposites.

Code	MG:MA (eq./eq.)	Gelation (%)
UPRC$_a$	1:2	89.05
UPRC$_b$	1:3	95.45
UPRC$_c$	1:4	95.49
UPRC$_d$	1:5	94.18

Table 3 displays the density of the UPRC$_{a-d}$ nanocomposites prepared by the UV curing technology of UPR based palm oil and reinforced by kenaf fiber, with different weight percentage gains (WPGs). WPGs used for the fabricated formulation were ranged from 6.25% to 14.38%. In general, the densities of UPRC$_{a-d}$ nanocomposites showed similar somehow lower density values based on the given void % values ranged from 9.4 ($\pm$0.46) in the case of UPRC$_c$ up to 12.4 ($\pm$0.52) in the case of UPRC$_d$. The other compositions UPRC$_a$ and UPRC$_b$ gave void values as 11.7 ($\pm$0.34) and 11.1 ($\pm$0.39) respectively. This can be attributed to the incorporation of lignocellulosic fiber reinforced with lower densities in the preparation of composites [16]. Table 3 also shows the T$_d$ and M$_d$ values for the same mentioned above composite materials. On comparison between the given values, it was found that, M$_d$ showed lower values than T$_d$ under the same composition of each formulation [17]. The decrease in density could be attributed to the presence of void in the composites, which may be located in the interface between the fiber and matrix. In addition, the void may be located in the matrix and the fiber [16].

Table 3: Td and Md Values and Void Contents of the UPRC$_{a-d}$ Composites.

Code	*WPG	T$_d$ (g/cm³)	M$_d$ (g/cm³)	Void (%)
UPRC$_a$	6.25	1.24	1.11	11.7 ($\pm$0.34)
UPRC$_b$	12.48	1.20	1.08	11.1 ($\pm$0.39)
UPRC$_c$	14.38	1.16	1.06	9.4 ($\pm$0.46)
UPRC$_d$	11.98	1.18	1.05	12.4 ($\pm$0.52)

* WPGs: weight percentage gains

Molar percentage of different solvents uptake of the UPRC$_{a-d}$ composites with different WPGs has been produced in two different solvents including DMF and toluene. The values of n and k were calculated via linear regression analysis. The n and k values of the fabricated nanocomposites are given in Table 4. The reported n values are ranged from 0.52 – 0.56 in DMF and from 0.54 – 0.61 in toluene. As reported in the literature, the mechanism of the sorption process can be attributed to Fickian when the n value lies close to 0.5. On the other hand, the sorption process is referred to non-Fickian if the n value lies close to 1 [18]. Furthermore, it is reported that solubility parameters of lignocellulosic-based nanocomposites, follow the diffusion mechanism as has been given as Fickian when the value of n is closely to 0.5 [19]. Therefore, on te based of the observed n values, the mechanism of sorption is referred as Fickian. By another meaning, sorption kinetics of the UPRC$_{a-d}$ composites depend on the concentration of the solvent and time. It is observed that k value did not exhibit any particular trend as we saw for the k value [20].

Table 4. n and k Values for the UPRC$_{a-d}$ composites in DMF and Toluene.

Code	DMF		Toluene	
	N	k (x10⁻³)	N	k (x10⁻³)
UPRC$_a$	0.52	4.58	0.54	6.43
UPRC$_b$	0.53	3.97	0.57	8.94
UPRC$_c$	0.56	5.61	0.58	6.82
UPRC$_d$	0.55	8.24	0.61	4.68

3. Methodologies

3.1. Materials and Solvents

Kenaf fiber obtained from National Tobacco Board, Malaysia. Palm oil was purchased from local market in Malaysia, maleic anhydride (Fluka, Analytical $\geq$ 98.00% mp = 52-54 ℃), glycerol reagent plus (Sigma, $\geq$ 99.00% FW = 92.09, FP = 160 ℃, bp = 182 ℃ / 20 mmHg, d = 1.262g/cm³), 2-methylimidazole (Fluka, $\geq$ 98%, mp = 144 – 146 ℃) sodium hydroxide (Systerm company $\geq$ 99.00%), molecular sieve (Fluka, type 3A) styrene (Sigma-Aldrich, $\geq$ 99.00% d = 0.909), pyridine (Aldrich, $\geq$ 99%, bp = 115.2 ℃, d = 0.9819), hydroquinone (Systerm company, > 99%, mp = 171 - 175 ℃) and photoinitiator IRGACURE 1800 was supplied by (Ciba Specialty, Singapore) Pte. Ltd. All of the materials mentioned before were used without purification. Solvents with different solubility parameters and of analytical grade, such as toluene [8.9 (cal/cm³)$^{1/2}$], acetone [9.9 (cal/cm³)$^{1/2}$], N,N`-dimethylformamide [DMF; 12.1 (cal/cm³)$^{1/2}$], and ethanol [12.7 (cal/cm³)$^{1/2}$] [21] were used.

3.2. Synthesis of ultraviolet-cured unsaturated polyester resins

3.2.1. Monomer preparation [16]

Palm oil (162.26 g) was mixed with 0.1 % sodium hydroxide and placed in a 500 ml reaction flask and stirred the reaction mixture using

2000 rpm/min mechanical stirrer. The dry nitrogen inlet and outlet was connected to the reaction container. 27.74 ml of glycerol at a molar ratio of 1:2.2 was put inside the dropping funnel connected to the reaction flask and was added drop-wise. In the first five minutes, nitrogen gas was made to flow faster, subsequently, the flow was at a decreased rate for rest of the experiment. The reaction mixture was heated to 220–240 ℃ for three to four hours. Subsequently, a small amount of the sample was taken out by a glass rod to test its solubility in ethanol. The test for solubility were continued until the collected solution had no emulsion or white spots. At that stage, the mixture was cooled in ice water, and transferred into a beaker and sealed for the next experiment.

3.2.2. Polymers matrices preparation [16]

In a round-bottomed reaction flask with a mechanical stirrer (2000 rpm/min), 1 eq. of monoglyceride (MG) monomer was heated until it melts. Then, a mixture of 0.15 % of hydroquinone was added to mitigate possible polymerization reactions. Varying amounts of maleic anhydride (MA) (2–5 eq.) were introduced to the reaction mixture with constant stirring, with 2-methylimidazole as a catalyst. Subsequently, the mixture was stirred at a temperature less than 90 ℃ for five hours, after which it was cooled down to get a dark viscous liquid. The resulting polymers were dried and poured into a beaker *and* sealed for the next experiment.

3.3. Photo-Fabrication of UPR Composites
3.3.1. Fiber Mat Preparation

Kenaf fibers were combed via a laboratory Carding Machine-337A, (MESDAN, Italy). Then, fibers were formed into a mat (20 x 20 cm²) in a deckle box through the aforementioned procedure [22] and dried in an oven at 105 ℃ for 24 hours. Afterward, mats were passed through a Needle Punch Testing Machine model (SNP-50), Shoou Shyng Machinery co., Ltd. with a speed of 200 strokes/min. Finally, the needle-punched mats were pressed using a hot press Gotech Testing Machine Inc model GT-7014–100 (2 min, 500 kg/cm², 100℃) and the thickness of the mats were appropriated to ~1 mm.

3.3.2. Preparation of Composites [23]

The previously prepared polymer matrices (100 g) were mixed with styrene (30 ml, 30%) and a photoinitiator (IRGACURE 1800, 3 g, 3%). The mixture was stirred for ten minutes by a mechanical stirrer, evacuated under vacuum (30 mmHg, 20 min.) to remove air bubbles, if there were any. The whole mixture was then poured onto a fiber mat impregnated with a resin mixture. If any air bubbles were still there, they were removed by a hand roller. The mat was then sandwiched between two glass panels. After impregnation, mats were passed through a 1ST UV machine (model M20-1-Tr-SLC) for twenty passes (each pass 28.3 x 10 uW/Cm²) at a conveyor speed of 5 m/min. The machine consisted of a medium pressure mercury arc lamp with UV radiation wavenumber of 180–450 nm. Table 1 includes all the symbols and the chemical compositions for the synthesized UPR /composites.

3.4. Void Content Determination

Each biofiber composite's void content was determined according to ASTM D 2734–70 with six replicates. First, the theoretical density (Td; g/cm³) of each sample was assessed and compared with the measured density. The missing fraction of each sample was considered the void content. T$_d$ of the UPRC and the void content were calculated via the following equation:

$$T_d = 100 / [(\%UPR/ \rho\ UPR) + (\%\ styrene/ \rho\ styrene) + (\%KF/ \rho\ KF)]$$

Where %UPR represents the weight percentage of UPR, ρ UPR the density of UPR (g/cm³), % styrene styrene weight percentage, ρ styrene styrene density (1.12 g/cm³), %KF KF's weight percentage, and ρ KF KF's density (g/cm³)

3.5. Density Determination

A Pyrex Gay–Lussac bottle (a density bottle or specific gravity bottle) of 25 ml capacity was used to determine the density of KF. Toluene was used as the medium to measure KF's density since it was a non-swelling agent for most of the lignocellulosic materials. The equations shown below were employed to gauge KF's density. The

composites' density was determined by the measurement of its dimensions and weight:

$$SG_T = (W_3 - W_1) / (W_2 - W_1)$$

$$SG_{KF} = \{(W_4 - W_1) / [(W_3 - W_1) - (W_5 - W_4)]\} \times SG_T$$

Where SG_T represents the specific gravity of toluene, the empty density bottle weight (g) is W_1, density bottle filled with distilled water (g) is W_2 and density bottle filled with toluene (g) is W_3. SG_{KF} the specific gravity of KF, W_4 the weight of the density bottle filled with KF (one-third full; g), and W_5 the weight of the density bottle filled with KF and toluene (g). The void content was determined as follows:

$$\text{Void content } \% = [(T_d - M_d) / T_d] \times 100$$

Where T_d represents the theoretical density and M_d the determined density (both in g/cm^3).

3.6. Swelling Test

Where Pre-dried UPRC$_{a-d}$ samples of 3 cm x 0.8 cm x 0.5 cm (length x width x thickness) dimensions were immersed in various solvents. The mass and thickness changes were examined regularly till they maintained constancy. Each sample's surface was dried with absorbent paper before being weighted, after which they were rapidly immersed in the corresponding solvent. This process had to be less than 30 seconds to evade solvent evaporation.

The solvent molecules observed to present in two states in the composites, which were untethered molecules in the cavities and tethered molecules with the appropriate constituents in the composites. Therefore, every composite's void content should have been evaluated to obtain the actual absorption under the conjecture that the solvent molecules in the cavities were untethered. The untethered solvent molecules in the cavity were adjusted for all of the sorption studies carried out according to the predetermined void contents. The equation used in calculations for solvent absorption is shown below:

$$M_s \text{ (g)} = p_s \times [V - (\text{void} \times V)]$$

Where M_s represents the mass of solvent absorbed at equilibrium swelling (g), p_s corresponds to solvent density, and V is the volume of the solvent absorbed.

The sorption mode (Fickian or nonFickian) determination and mechanism elucidation were accomplished by fitting the data in the following equation [24- 26]:

$$\text{Log } Q_t / Q = \text{Log } k + n \text{ Log } t$$

Here Q_t is the molar percentage of solvent absorbed at time t, Q' is the molar percentage of solvent absorbed at equilibrium (corrected), and n the slope of the graph Log Q_t / Q against Log t, k is a constant.

n and k values were calculated by linear regression analysis [27–29]. The k value refers to the extent of the polymer–solvent interaction [24] while the n value signifies the mode of the sorption mechanism. The diffusion coefficient or diffusivity (D) of the solvent in a composite could be calculated by the following equation [28–30]:

$$D = \pi / 16(h\theta = Q')^2$$

Where, h represents the samples' initial thickness and θ the slope of the graph of Q_t against $t^{1/2}$ before 50% sorption.

The sorption coefficient (S) correlates with the solvent's maximum sorption, obtainable from the ratio of the weight of the solvent absorbed at the equilibrium state to the polymer's initial weight [26]. S of the UPRC was calculated via the following equation [28, 29]:

$$S = M_s = M_p$$

Where M_s represents the mass of solvent absorbed at equilibrium swelling (g) and M_p the composite's mass at the initial state (g).

UPRC permeability could be expressed by permeability coefficient (P), which was calculated by the following equation [28, 29]:

$$P = DS$$

The swelling coefficient (α) was obtained by the next equation. The solubility parameter of each series of UPRC was obtained when the maximum swelling was achieved [27, 31]:

$$\alpha = (M_s / M_p) \times (1 / p_s)$$

Where M_s stands for the mass of the solvent in the swollen sample at equilibrium (g), M_p the composite's mass at the initial state (g), and p_s the density of the respective solvent (g/cm^3).

Each type of composite's χ was determined by the equation shown next [27, 31]:

$$\chi = \beta + V_s [(\delta p - \delta s)^2 / RT]$$

Where β represents the lattice constant (0.34), V_s the molar volume of the solvent (cm^3/mol), δp the composite's solubility parameter [(cal/cm^3)$^{1/2}$], δs is the solvent's solubility parameter [(cal/cm^3)$^{1/2}$], R the gas constant (1.983 cal mol^{-1} K^{-1}), and T the temperature (K).

4. Conclusions

To conclude, gel fraction in the fiber composite increased with increasing amount of MA up to the ratio of MG to MA was 1:4 (eq./eq.) for UPRC$_c$, but it decreased for formulation of 1:5 (eq./eq.). The drop was attributed to the pre reaction of the unsaturated groups during the preparation of the resin. The WPGs % used for the fabricated formulation were ranged from 6.25% up to 14.38%. Similar to gel fraction the formulation 1:5 (eq./eq.) nanocomposite wpg exhibited an aberration to the trend of increase in WPG %. The measured densities of all nanocomposites were lower than theoretical densities. The densities exhibited a steady trend of drop with UPRC$_a$ the lowest and UPRC$_d$ the lowest measured density. The decrease in density could be attributed to the presence of void in the composites, located in the interface between the fiber and matrix. The nanocomposite with lowest density had highest void content. n values for nanocomposites are ranged from 0.52 – 0.56 in DMF and from 0.54 – 0.61 in toluene. The n values are indicative of Fickian sorption mechanism. The amount of the solvent exhibit greater effect on properties of polyesters. This effect is presumed that there may be some structural modification.

Conflicts of Interest: "The authors declare no conflict of interest."

References

[1] B. N. Regnier and B. Mortaigne. Analysis by pyrolysis/gas chromatography/mass spectrometry of glass fibre/vinylester thermal degradation products. *Polymer Degradation and Stability,* **1995,** *49*, 419-428. https://doi.org/10.1016/0141-3910(95)00129-A

[2] B. Mortaigne, S. Bourbigot, M. Le Bras, G. Cordellier, A. Baudry and J. Dufay. Fire behaviour related to the thermal degradation of unsaturated polyesters. *Polymer Degradation and Stability,* **1999**, *64*, 443-448. https://doi.org/10.1016/S0141-3910(98)00149-9

[3] Y. Li, Y. W. Mai, L. Ye. Sisal fibre and its composites: a review of recent developments. *Composites Science and Technology*, **2000,** *60*, 2037-2055. https://doi.org/10.1016/S0266-3538(00)00101-9

[4] B. N. Dash, A. K. Rana, H. K. Mishra, S. K. Nayak and S. S. Tripathy. Novel low-cost jute–polyester composites. III. Weathering and thermal behavior. *J Appl Polym Sci*, **2000**, *78*, 1671-1679. https://doi.org/10.1002/1097-4628(20001128)78:9<1671::AID-APP130>3.0.CO;2-8

[5] L. Y. Mwaikambo and M. P. Ansell. Chemical modification of hemp, sisal, jute, and kapok fibers by alkalization. *J Appl Polym Sci,* **2000,** *84,* 2222-2234 https://doi.org/10.1002/app.10460

[6] A O'Donnell, M.A Dweib and R.P Wool. Natural fiber composites with plant oil-based resin. *Composites Science and Technology,* **2004,** *64,* 1135-1145. https://doi.org/10.1016/j.compscitech.2003.09.024

[7] W. D. Bascom, Interphase in fiber reinforced composites. International encyclopedia of composites, VCH New York, 1990.

[8] S. M. Lung, K. J. Kyo and W. Jingshen. Effects of coupling agent concentration and hygrothermal ageing on the fracture behaviour of glass woven fabric-reinforced vinyl ester laminates. *Polym Polym Compos,* **1997**, *5,* 165-175. http://hdl.handle.net/1783.1/47758

[9] H. Mahiou, and A. Béakou. Modelling of interfacial effects on the mechanical properties of fibre-reinforced composites. *Composites Part A: Applied Science and Manufacturing,* **1998,** *29*, 1035-1048. https://doi.org/10.1016/S1359-835X(98)00090-6

[10] R. T. Graf, J. L. Koenig and H. Ishida. The Influence of Interfacial Structure on the Flexural Strength of E-glass Reinforced Polyester. *The Journal of Adhesion*, **1983**, *16,* 97-113. https://doi.org/10.1080/00218468308074908

[11] Y. Suzuki, Z. Maekawa, H. Hamada, A. Yokoyama, T. Sugihara and M. Hojo. Influence of silane coupling agents on interlaminar fracture in glass fibre fabric reinforced unsaturated polyester laminates. *J Mater Sci*, **1993**, *28,* 1725–1732. https://doi.org/10.1007/BF00595738

[12] A. Sjögren, R. Joffe, L. Berglund and E Mäder. Effects of fibre coating (size) on properties of glass fibre/vinyl ester composites. *Composites Part A: Applied Science and Manufacturing,* **1999,** *30,* 1009-1015. https://doi.org/10.1016/S1359-835X(99)00005-6

[13] E. Rodríguez, R. Petrucci, D. Puglia, J. M. Kenny and A.Vázquez. Characterization of Composites Based on Natural and Glass Fibers Obtained by Vacuum Infusion. *J Comp Mater,* **2005,** *39*, 265-282. https://doi.org/10.1177/0021998305046450

[14] O. A. S. Adeakin, V. A. Popoola and K. K. Ajekwene. Polymer - Solvent Relation: Swelling and Fibre Morphology. *IOSR Journal of Polymer and Textile Engineering (IOSR-JPTE)* **2017,** 4(2), 27-28. http://doi:10.9790/019X-04022728

[15] H. Mahmoud, G. S. Tay and H. D. Rozman. A Preliminary Study on Ultraviolet Radiation-Cured Unsaturated Polyester Resin Based on Palm Oil. *Polymer-Plastics Technology and Engineering,* **2011,** *50,* 573-580. https://doi.org/10.1080/03602559.2010.543740

[16] C. A. S. Hill and H. P. S. Abdul Khalil. Effect of fiber treatments on mechanical properties of coir or oil palm fiber reinforced polyester composites. *J Appl Polym Sci,* **2000,** *78,* 1685-1697. https://doi.org/10.1002/1097-4628(20001128)78:9<1685::AID-APP150>3.0.CO;2-U

[17] F. Zhang, T. Endo, W. Qiu, L. Yang and T. Hirotsu. Preparation and mechanical properties of composite of fibrous cellulose and maleated polyethylene. *J Appl Polym Sci,* **2002,** *84,*1971-1980. https://doi.org/10.1002/app.10428

[18] G. Unnikrishnan and S. Thomas. Diffusion and transport of aromatic hydrocarbons through natural rubber," *Polymer,* **1994**, *35,* 5504-5510. https://doi.org/10.1016/S0032-3861(05)80015-1

[19] M. S. Sreekalaa, M. G. Kumarana and S. Thomas. Water sorption in oil palm fiber reinforced phenol formaldehyde composites. *Composites Part A: Applied Science and Manufacturing,* **2002,** *33,* 763-777. https://doi.org/10.1016/S1359-835X(02)00032-5

[20] U. S. Aithal. and T. M. Aminabhavi, "Molecular transport of some industrial solvents through a polyurethane membrane," J Appl Polym Sci, **1991,** *42,* 2837-2844. https://doi.org/10.1002/app.1991.070421023

[21] F. Grundert, and B. A. Wolf, In Polymer Handbook; Brandrup, J, Immergut EH, Eds.; Wiley New York, **1989**, p VII/173.

[22] H. D. Rozman M. A. Faiza and R. N. Kumar. A Preliminary Study on Ultraviolet Radiation–Cured Biofiber Composites from Oil Palm Empty Fruit Bunch. *Polymer-Plastics Technology and Engineering*, **2008,** *47*, 358-362. https://doi.org/10.1080/03602550801897414

[23] M. A. Hussein, G. S. Tay, H. D. Rozman. Photo-fabricated unsaturated polyester resin composites reinforced by kenaf fibers, synthesis and characterization. *J Appl. Polym. Sci.,* **2012,** *123,* 968-976. https://doi.org/10.1002/app.34681

[24] S.B. Harogoppad and T.M. Aminabhavi. Sorption and transport of aqueous salt solutions of acetates, acetic and monochloroacetic acids in polyurethane. *Polymer,* **1990,** *31,* 2346-2352. https://doi.org/10.1016/0032-3861(90)90323-Q

[25] G. Unnikrishnan and S. Thomas. Diffusion and transport of aromatic hydrocarbons through natural rubber. *Polymer,* **1994**, *35,* 5504-5510. https://doi.org/10.1016/S0032-3861(05)80015-1

[26] G. S. Tay and H. D. Rozman. Swelling properties of chemically modified oil palm empty fruit bunch based polyurethane composites. *J Appl Polym Sci,* **2008,** *108*, 995-1004 https://doi.org/10.1002/app.27598

[27] S. Desai, I. M. Thakore and S. Devi. Effect of crosslink density on transport of industrial solvents through polyether based polyurethanes. *Polym Int.,* **1998,** *47,* 172-178. https://doi.org/10.1002/(SICI)1097-0126(1998100)47:2<172::AID-PI43>3.0.CO;2-2

[28] M.S. Sreekala, M.G. Kumaran, S. Thomas. Water sorption in oil palm fiber reinforced phenol formaldehyde composites. *Composites Part A: Applied Science and Manufacturing,* **2002,** *33,* 763-777. https://doi.org/10.1016/S1359-835X(02)00032-5

[29] M.S. Sreekala and S. Thomas. Effect of fibre surface modification on water-sorption characteristics of oil palm fibres. *Composites Science and Technology,* **2003,** *63,* 861-869. https://doi.org/10.1016/S0266-3538(02)00270-1

[30] U. S. Aithal. and T. M. Aminabhavi. Molecular transport of some industrial solvents through a polyurethane membrane. *J Appl Polym Sci,* **1991,** *42,* 2837-2844. https://doi.org/10.1002/app.1991.070421023

[31] S. L. Rosen, "Linear viscoelasticity, Chapter XVIII, Fundamental Principles of Polymeric Materials, 2nd Ed., John Wiley and Sons, New